Indian J Phys (May 2016) 90(5):563–575
DOI 10.1007/s12648-015-0777-6

ORIGINAL PAPER

Electromechanical instability of nanobridge in ionic liquid electrolyte media: influence of electrical double layer, dispersion forces and size effect

I Karimipour[1], A Kanani[2], A Koochi[3], M Keivani[4] and M Abadyan[3]*

[1]Faculty of Engineering, Shahrekord University, Shahrekord, Iran

[2]Ionizing and Non-Ionizing Radiation Protection Research Center, Paramedical Sciences School, Shiraz University of Medical Sciences, Shiraz, Iran

[3]Shahrekord Branch, Islamic Azad University, Shahrekord, Iran

[4]Shahrekord University of Medical Sciences, Shahrekord, Iran

Received: 07 June 2015 / Accepted: 28 August 2015 / Published online: 7 October 2015

Abstract: In this paper, the electromechanical response and instability of the nanobridge immersed in ionic electrolyte media is investigated. The electrochemical force field is determined using double-layer theory and linearized Poisson–Boltzmann equation. The presence of dispersion forces, i.e., Casimir and van der Waals attractions are incorporated considering the correction due to the presence of liquid media between the interacting surfaces (three-layer model). The strain gradient elasticity is employed to model the size-dependent structural behavior of the nanobridge. To solve the nonlinear constitutive equation of the system, three approaches, e.g., the Rayleigh–Ritz method, Lumped parameter model and the numerical solution method are employed. Impacts of the dispersion forces and size effect on the instability characteristics as well as the effects of ion concentration and potential ratio are discussed.

Keywords: Beam-type nanobridge; Electromechanical pull-in instability; Ionic liquid electrolyte; Electrical double layer; Dispersion forces; Size effect

PACS Nos.: 85.85.+j; 46.32.+x; 46.70.−p; 77.65.−j; 47.61.Fg

1. Introduction

With recent advances in nanotechnology, beam-type nanobridges are increasingly used in various engineering and science branches, i.e., mechanics, chemistry, optics, biology, electronics [1]. This miniature element is one of the most essential electromechanical structural components that is highly potential for developing nanoscale resonators [2], switches [3], memories [4] and sensors [5]. A typical nanobridge is constructed from a movable conductive beam, which can be excited via applying electrical force field. The electrical stimulation results in deflection, vibration or actuation of the movable component, depending on the system design. Generally, when the applied voltage exceeds its critical value, the pull-in instability occurs and the system suddenly fails. Prediction and simulation of the electromechanical response and stability of nanobridge are very crucial for reliable design and fabrication of nanodevices; hence, many researchers have studied the pull-in behavior of these ultra-small structures [6–9].

Recently, microelectromechanical/nanoelectromechanical systems (MEMS/NEMS) have been widely considered for in-liquid applications especially in biological, chemical and electronic sciences. Some of the promising applications of MEMS/NEMS in bio-fluid include developing sensors and manipulators for cellular handling, bio-component characterization, device motion, DNA manipulation, bio-mimetic cilia, drug delivery, etc. [10–13]. Besides biology, nanodevices such as actuators, probes, tweezers, valves are employed as precise instruments operated in

*Corresponding author, E-mail: abadyan@yahoo.com

ionic liquid media [14]. Moreover, usages of liquid-immersed MEMS/NEMS have great potentials in developing supercapacitors, fuel cells, batteries, filters, microdensitometer, micropump/nanopump, active microfluidic devices and atomic force microscopy [14–17]. In this regard some researchers have investigated the mechanical behavior of MEMS/NEMS in liquid environment. Oh et al. [12] have fabricated and characterized the oscillating bio-mimetic microfluidic device that mimics biological cilia for manipulation of microfluidics. Maali et al. [18] have attempted to measure the influence of the fluid motion on the oscillating behavior of ultra-small cantilever beams immersed in viscous fluids. Yang and Zhao [19] have investigated the influences of hydration force on the stability of solid film in a very thin solid-on-liquid structure. The hydration forces become very strong at short range and are particularly important for determining the magnitude of the adhesion between two surfaces or interaction energy due to hydration-induced layering of liquid molecules close to a solid film surface [19]. The pull-in performance of electrostatic parallel-plate actuators in liquid solutions has been studied by Rollier et al. [10]. They have claimed that the pull-in deflection of the actuators can be suppressed in liquid. Only few works [14, 17, 20] have focused on the pull-in behavior of liquid-immersed NEMS in ionic media. In ionic electrolyte media, the electrochemical field is characterized by double-layer interaction [14, 17, 20].The double layer appears on the surface of an electrode if the electrode is exposed to ionic electrolyte fluid. Indeed, the double-layer concept implies the presence of two parallel layers of electrical charges surrounding the electrode surface. A simple lumped model for calculating the pull-in voltage of electrostatic actuators in ionic liquid electrolytes has been presented by Boyd and Kim [14]. They have incorporated the effect of double-layer electrochemical force in the pull-in model by solving the linearized Poisson–Boltzmann equation. In another work, Boyd and Lee [20] have modified their model with a distributed parameter model in order to achieve more accurate results. The electromechanical behavior and frequency response of an inter-digitated silicon comb-drive actuator in various ionic liquids has been investigated by Sounart et al. [17]. They have presented a theoretical model that predicts the characteristic actuation frequency of the system. Noghrehabadi et al. [21] have theoretically investigated the static stability of cantilever nanobeams in a liquid electrolyte using a distributed force model. It should be noted that to the best knowledge of the authors, all the mentioned works have studied the cantilever NEMS, while no researcher has yet investigated the electromechanical performance of double-clamped NEMS bridges in electrolyte media. The present work aims to investigate the electromechanical response and pull-in instability of the electromechanical nanobridge immersed in ionic liquid electrolyte environment.

It is well established that the electromagnetic vacuum fluctuations, i.e., dispersion forces, can significantly affect the electromechanical performance of nanostructures. The dispersion forces between interacting bodies are generally explained as Casimir or van der Waals (vdW) attractions depending on the distance between the bodies. The effect of dispersion forces on the pull-in instability of nanoactuators operating in non-liquid environments (i.e., gas or vacuum) has been studied by previous researchers [22–30]. Herein, we examine the impact of dispersion forces on the pull-in instability of liquid-immersed nanobridge considering the corrections due to the presence of liquid media in between the electrodes.

A powerful method for study of nanoscale systems is molecular dynamics/mechanics. However, this method is very time consuming in modeling nanostructures with large number of interacting atoms such as nanobridge. To overcome this shortcoming, nanoscale continuum mechanic models are developed to investigate the electromechanical performance of nanostructures [20]. Since the elastic characteristics of materials in nanoscale may be size dependent [31–33], the applied models should be able to consider this size dependency in constitutive equations. The size dependency cannot be modeled by using classical continuum mechanics. In this regard, the non-classical theories such as strain gradient theory [33] have been developed to consider the size effect in theoretical continuum models. The strain gradient theory introduces additional elastic constants, i.e., three material length scale parameters, to interpret the size-dependent behavior of elastic solids. While some researchers have utilized strain gradient theory for analyzing the MEMS/NEMS pull-in instability in non-liquid environments (gas and vacuum) [34–42], none of them has investigated this phenomenon in liquid electrolyte media. In this work, the size-dependent pull-in instability of nanobridge immersed in liquid electrolytes has been investigated in the presence of vdW and Casimir forces. The electrochemical force field has been determined using double-layer theory and linearized Poisson–Boltzmann equation. The strain gradient theory in conjunction with Euler–Bernoulli beam model has been used to derive the nonlinear equilibrium equation of system incorporating the beam stretching effect. The Rayleigh–Ritz method (RRM) has been applied to solve the governing equation of the system. The obtained results have been compared with those of numerical method. Moreover, a lumped parameter model (LPM) has been developed to explain the influences of the electrical double layer, dispersion forces and size phenomenon on the stable performance of the anno-bridge.

2. Theoretical model

Figure 1 shows the schematic representation of the nanobridge which is constructed from a conductive double-clamped electrode suspended over another fix one (grounded electrode). The moveable electrode with a length of L, wide of b and thickness of h is considered. The total energy of the system is the summation of the stored strain energy and work of external forces.

2.1. Stored strain energy

By employing the strain gradient theory modified by Lam et al. [33], $\bar{U}$, the stored strain energy density in elastic materials is written as the following:

$$\bar{U} = \frac{1}{2}\left(\sigma_{ij}\varepsilon_{ij} + p_i\gamma_i + \tau^{(1)}_{ijk}\eta^{(1)}_{ijk} + m^s_{ij}\chi^s_{ij}\right) \tag{1}$$

in which

$$\varepsilon_{ij} = \frac{1}{2}\left(u_{i,j} + u_{j,i}\right) \tag{2}$$

$$\gamma_i = \varepsilon_{mm,i} \tag{3}$$

$$\eta^{(1)}_{ijk} = \frac{1}{3}\left(\varepsilon_{jk,i} + \varepsilon_{ki,j} + \varepsilon_{ij,k}\right) - \frac{1}{15}\left[\delta_{ij}\left(\varepsilon_{mm,k} + 2\varepsilon_{mk,m}\right) + \delta_{jk}\left(\varepsilon_{mm,i} + 2\varepsilon_{mi,m}\right) + \delta_{ki}\left(\varepsilon_{mm,j} + 2\varepsilon_{mj,m}\right)\right] \tag{4}$$

$$\chi^s_{ij} = \frac{1}{2}e_{jkl}u_{l,ki} \tag{5}$$

In above equations, $u_i, \gamma_i, \eta^{(1)}_{ijk}, \chi^s_{ij}, \delta_{ij}$ and e_{ijk} indicate components of displacement vector, dilatation gradient vector, deviatoric stretch gradient tensor, symmetric rotation gradient tensor, Kronecker delta and permutation symbol, respectively. Also $\sigma_{ij}, p_i, \tau^{(1)}_{ijk}, m^s_{ij}$, are components of Cauchy's stress and high order stress tensors, respectively, that are identified as [33]:

$$\sigma_{ij} = 2\mu\left(\varepsilon_{ij} + \frac{v}{1-2v}\varepsilon_{mm}\delta_{ij}\right) \tag{6}$$

$$p_i = 2\mu l_0^2\gamma_i \tag{7}$$

$$\tau^{(1)}_{ijk} = 2\mu l_1^2\eta^{(1)}_{ijk} \tag{8}$$

$$m^s_{ij} = 2\mu l_2^2\chi^s_{ij} \tag{9}$$

In the above equations, v and μ are Poisson's ratio and shear modulus, respectively. Also l_0, l_1 and l_2 are additional material length scale parameters which are related to dilatation gradient vector, deviatoric stretch gradient tensor and symmetric rotation gradient tensor. The material length scale parameters can be measured using experimental techniques, molecular dynamics, etc. Some experimental measurements evaluate the material length scale parameter of single-crystal and polycrystalline copper to be 12 and 5.84 μm, respectively [43, 44]. Also, the size-dependent behavior has been detected in some kinds of polymers [45]. For hardness measurement of bulk gold, it is found that the plastic length scale parameter (for indentation test and hardness behavior) of Au increases from 470 nm to 1.05 μm with increasing the Au film thickness from 500 nm to 2 μm [46]. Based on test results gathered via microhardness test, the plastic length scale parameter for metals such as Cu, Ag and Brass was determined in the range about 0.2–20 μm based on the crystallinity [47]. Using microbend testing method, the plastic intrinsic material length scale of 4 μm for copper and 5 μm for nickel were determined [48]. All these experiments imply that when the characteristic size (thickness, diameter, etc.) of a microelement/nanoelement is in the order of its intrinsic the material length scales (typically sub-micron), the material elastic constants highly depend on the element dimensions. Molecular dynamic simulations also could be used to compute the material length scale parameters of materials [49]. By comparing the results of size-dependent continuum theories with those of molecular dynamics, one can extract the size parameters [50].

Now, based on Euler–Bernoulli beam theory, the displacement field can be written as the following:

$$u_1 = -Z\frac{\partial W(X)}{\partial X}, \quad u_2 = 0, \quad u_3 = W(X) \tag{10}$$

where u_1, u_2, u_3 and W are the displacement field of the beam in the X, Y, Z directions and centerline beam displacement, respectively.

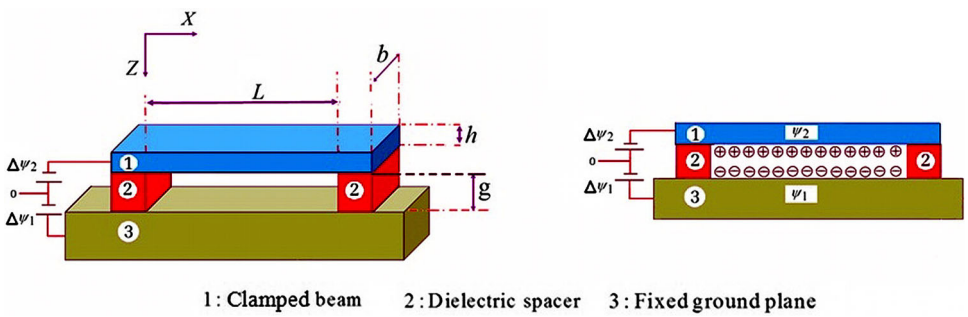

Fig. 1 Schematic representation of double-clamped nanobridge

By using Eq. (10) in conjunction with Eqs. (2)–(9), the stress and strain components are defined. By substituting the stress and strain components in Eq. (1), the energy density is obtained. Afterward, by integrating the energy density over the beam volume the bending strain energy, U_{bend}, is obtained as:

$$U_{\text{bend}} = \int_V \bar{U}\mathrm{d}V = \frac{1}{2}\int_0^L \left[\left(\text{EI} + 2\mu A l_0^2 + \frac{8}{15}\mu A l_1^2 + \mu A l_2^2\right)\left(\frac{\partial^2 W}{\partial X^2}\right)^2 + A\left(2\mu l_0^2 + \frac{4}{5}\mu l_1^2\right)\left(\frac{\partial^3 W}{\partial X^3}\right)^2\right]\mathrm{d}X \tag{11}$$

In above equation, I is second cross section moment around Y axis and A is the cross section area.

Besides the bending energy, the elastic stored energy due to the beam stretching should be taken into account. The stretching arises from resisting the double-clamped beam against the change in the length that is induced by the beam deflection. The stretching energy stored in the beam, U_{stretch}, due to axial forces can be written as [51]:

$$U_{\text{stretch}} = \frac{1}{2}\int_0^L F_a\left(\frac{\partial W}{\partial X}\right)^2 \mathrm{d}X \tag{12}$$

In the above equation, F_{a} is the axial resultant force associated with the mid-plane stretching. When nanobeam is in tension, the actual beam length L' becomes longer than the original length L. However, the beam is immovable at both ends of the nanobridge. Thus, an additional axial force occurs and can be expressed as:

$$F_{\text{a}} = \frac{\text{EA}}{L}(L' - L) \approx \frac{\text{EA}}{2L}\int_0^L \left(\frac{\partial W}{\partial X}\right)^2 \mathrm{d}X \tag{13}$$

By substituting Eq. (13) into Eq. (12), the elastic energy due to stretching is determined.

2.2. Work of external forces

The external forces are the summation of electrochemical and dispersion forces. Considering the distribution of external forces per unit length of the beam (f_{ext}), the work by the external forces, V_{ext}, can be obtained as:

$$V_{\text{ext}} = \int_0^L \int_0^W f_{\text{ext}}(X)\mathrm{d}W\mathrm{d}X = \int_0^L \int_0^W \left[f_{\text{EC}} + \begin{Bmatrix} f_{\text{Cas}} \\ f_{\text{vdW}} \end{Bmatrix}\right]\mathrm{d}W\mathrm{d}X \tag{14}$$

where f_{EC} is the electrochemical force which is the sum of the electrical force and chemical (or osmotic) force. In above relation the Casimir attraction per unit length, f_{Cas} and the vdW force per unit length, f_{vdW}, are considered corresponding to the gap distances. These forces are determined in the following subsections.

2.2.1. *Electrochemical force*

The electrochemical force is the sum of the electrical force F_{e} and chemical force F_{c} which can be written as Eqs. (15) and (16), respectively [20]:

$$F_{\text{e}} = -\frac{1}{2}\varepsilon\varepsilon_0|\nabla\psi|^2 \tag{15}$$

$$F_{\text{c}} = 2n_\infty K_B T b\left[\cosh\left(\frac{z_0 e\psi}{K_B T}\right) - 1\right] \tag{16}$$

where ε_0 is the permittivity of vacuum, ε is the relative permittivity of the dielectric medium, K_{B} is the Boltzmann constant, n_∞ is the bulk concentration, T is the absolute temperature, e is the electronic charge, z_0 is the absolute value of the valence, and b is the width of electrode. In the above equation ψ is the electric potential of the liquid-immersed electrodes which is the summation of applied potential and zeta potential for each electrode and can be obtained from the Poisson–Boltzmann equation as the following [20]:

$$\nabla^2\psi = \frac{2z_0 e n_\infty}{\varepsilon\varepsilon_0}\sinh\left(\frac{z_0 e\psi}{K_B T}\right) \tag{17}$$

For small potentials by solving the linearized form of Eq. (17), the total electrochemical force is obtained as:

$$f_{\text{EC}} = F_e + F_c = \frac{b\varepsilon\varepsilon_0\kappa^2\psi_1^2}{2\sinh^2[\kappa(g - W(X))]} \times \left(2\frac{\psi_2}{\psi_1}\cosh[\kappa(g - W(X))] - 1 - \left(\frac{\psi_2}{\psi_1}\right)^2\right) \tag{18}$$

where g is the initial gap between two electrodes, $\kappa^2 = 2e^2 z_0^2 n_\infty/\varepsilon\varepsilon_0 K_B T$ and $1/\kappa$ is the Debye length. The electrochemical force can be attractive or repulsive, depending on the dominant parameters.

2.2.2. *Dispersion force*

It should be mentioned that the strength of nanoscale forces between two surfaces interacting across a non-vacuum media in between them is affected by the characteristics of the intervening media. In this case a three-layer approach should be considered for determining the dispersion forces [52, 53]. The dispersion forces per unit length of the nanobridge are defined considering the vdW and Casimir force regimes. Based on what mentioned, two interaction regimes can be defined:

First, the large separation regime in which the Casimir force is dominant (typically above several tens of nanometers [54–56]). The Casimir energy due to a quantum field is the sum of the zero point energies of the quantum field [52]. The Casimir force between two perfectly conducting planar geometries separated by medium with constant refractive index is calculated as a limit case of a three-layer model using the piston approach [55]. Using piston approach, the Casimir attraction per unit length, f_{Cas}, of conductive electrode of nanobridge operating in a liquid media is obtained as [52]:

$$f_{\mathrm{Cas}} = \frac{\pi^2 \hbar b}{240 n (g - W(X))^4} \tag{19}$$

where $\hbar = 1.055 \times 10^{-34}$ Js is Planck's constant divided by 2π and n is the refractive index of fluid, respectively.

The second regime is the small separation regime (typically below several tens of nanometers [54–56]), in which the vdW force is the dominant attraction. In this case, the attraction between two ideal surfaces is proportional to the inverse cube of the separation. Considering three-layer interaction (two metals separated by liquid medium), the vdW force per unit length, f_{vdW}, of the movable conductive electrode of the nanobridge is [53]:

$$f_{vdW} = \frac{\bar{A}(n) b}{6\pi (g - W(X))^3} \tag{20}$$

where $\bar{A}(n)$ is the Hamaker constant for three-layer interaction which is a function of refractive index (n) of the liquid media. For conductive metals (such as Ag, Cu, Au, etc.) interacting across water-based media, the Hamaker constant is about 10–40 $\times 10^{-20}$ J [53]. It should be noted that the van der Waals interaction potential is largely insensitive to variations in electrolyte concentration and pH, and so may be considered as fixed in a first approximation [53].

2.3. Dimensionless total energy

By using Eqs. (11), (12) and (14) the total energy of system can be summarized as:

$$\begin{aligned} \Pi &= U_{\mathrm{bend}} + U_{\mathrm{stretch}} - V_{\mathrm{ext}} \\ &= \frac{1}{2}\int_0^L \left[\left(\mathrm{EI} + 2\mu A \left(l_0^2 + \frac{8}{15} l_1^2 + l_2^2 \right) \right) \left(\frac{\mathrm{d}^2 W}{\mathrm{d}X^2} \right)^2 \right. \\ &\quad \left. + A\mu \left(2 l_0^2 + \frac{4}{5} l_1^2 \right) \left(\frac{\mathrm{d}^3 W}{\mathrm{d}X^3} \right)^2 \right] \mathrm{d}X \\ &\quad + \frac{1}{2}\int_0^L F_{\mathrm{a}} \left(\frac{\mathrm{d}W}{\mathrm{d}X} \right)^2 \mathrm{d}X - \int_0^L f_{\mathrm{ext}} W(X) \mathrm{d}X \end{aligned} \tag{21}$$

Now, by using the substitutions $x = X/L$ and $w = W/g$ the non-dimensional total energy can be explained as:

$$\begin{aligned} \bar{\Pi} &= \frac{1}{2}\int_0^1 \left[D_1 \left(\frac{\mathrm{d}^2 w}{\mathrm{d}x^2} \right)^2 + D_2 \left(\frac{\mathrm{d}^3 w}{\mathrm{d}x^3} \right)^2 \right] \mathrm{d}x \\ &\quad + \frac{1}{2}\int_0^1 \eta \left[\int_0^1 \left(\frac{\mathrm{d}w}{\mathrm{d}x} \right)^2 \mathrm{d}x \right] \left(\frac{\mathrm{d}w}{\mathrm{d}x} \right)^2 \mathrm{d}x \\ &\quad - \int_0^1 \left[\frac{\alpha_m}{(1 - w(x))^m} - \frac{\beta^2 \{ 2\lambda \cosh(\xi_0 (1 - w(x))) - (1 + \lambda^2) \}}{2 \sinh^2 (\xi_0 (1 - w(x)))} \right] w(x) \mathrm{d}x \end{aligned} \tag{22}$$

where the dimensionless parameters are identified as the following:

$$\alpha_m = \begin{cases} \frac{\bar{A}(n) b L^4}{6\pi g^4 \mathrm{EI}} & \text{vdW interaction } (m = 3) \\ \frac{\pi^2 \hbar b L^4}{240 n g^5 \mathrm{EI}} & \text{Casimir interaction } (m = 4) \end{cases} \tag{23}$$

$$\beta = \psi_1 \sqrt{\frac{b \varepsilon \varepsilon_0 \kappa^2 L^4}{g}} \tag{24}$$

$$\eta = 6 \left(\frac{g}{h} \right)^2 \tag{25}$$

$$\mu_s = \frac{12\mu}{E \left(\frac{h}{l_2} \right)^2} \tag{26}$$

$$\lambda = \frac{\psi_2}{\psi_1} \tag{27}$$

$$\xi_0 = \kappa g \tag{28}$$

$$D_1 = 1 + \frac{\mu_s}{15} \left(30 \left(\frac{l_0}{l_2} \right)^2 + 8 \left(\frac{l_1}{l_2} \right)^2 + 15 \right) \tag{29}$$

$$D_2 = \frac{\mu_s}{30 \left(\frac{L}{h} \right)^2} \left(5 \left(\frac{l_0}{l_2} \right)^2 + 2 \left(\frac{l_1}{l_2} \right)^2 \right) \tag{30}$$

In above relations, β, μ_s, α_m and ξ_0 interpret the dimensionless values of beam electrode voltage, size effect, dispersion forces and bulk ion concentration. The dimensionless parameter λ indicates the ratio of potential on the ground electrode over the beam electrode.

Note that the effect of hydration forces is not incorporated in the theoretical double-layer model. Indeed, the classical double-layer theory is a continuum theory that does not consider the discrete molecular nature of the surfaces that can become important at small distances. It has long been postulated that a modified water structure exists at solid–water interfaces. In fact, hydrophobicity is a manifestation of water structure at surfaces. For interfaces in aqueous media, the predominant effect is attributed to the hydration of the adsorbed counterions and ionic functional groups in the surface [19]. As the close-enough

interacting surfaces, some dehydration of the ions and surface would have to occur, resulting in an increase in the free energy and hence a repulsion [19]. This phenomenon is usually known as hydration force. So the hydration force should be taken into account when the liquid medium between two interacting surfaces is only few molecular diameters in width. Since, the hydration forces become important at small gaps (<5 nm) [19], the present model should be corrected for nanobridges with<5 nm gap in order to incorporate the hydration forces.

3. Solution methods

3.1. Rayleigh–Ritz method (RRM)

To solve the governing equation of the systems by Rayleigh–Ritz method, the displacement is expressed as a linear combination of a complete set of independent basis functions $\varphi_i(x)$ in the form of:

$$w(x) = \sum_{i=1}^{n} q_i \phi_i(x) \tag{31}$$

where the index i refers to the number of terms included in the simulation. We have used the free vibration mode shapes of the nanobeam as basic functions in the Rayleigh–Ritz procedure. The mode shapes of clamped nanobeam (based on classical theory) can be expressed as [57]:

$$\phi_i(x) = \cosh(\lambda_i x) - \cos(\lambda_i x) - \frac{\cosh(\lambda_i) - \cos(\lambda_i)}{\sinh(\lambda_i) - \sin(\lambda_i)} (\sinh(\lambda_i x) - \sin(\lambda_i x)) \tag{32}$$

where λ_i is the ith root of characteristic equation of clamped–clamped beams ($\lambda_1 = 4.73$, $\lambda_2 = 7.8532$). In the equilibrium point the following relation must be satisfied:

$$\frac{\partial \bar{\Pi}}{\partial q_i} = 0 \quad i = 0, 1, \ldots, N \tag{33}$$

This leads to a system of algebraic equation which can be solved numerically to obtain the final solution. Using Taylor expansion for electrostatic and dispersion force, substituting Eqs. (22), (31) and (32) into Eq. (33), assuming the orthogonality of $\varphi_i(x)$ and then following some straightforward mathematical operations, a system of algebraic equation can be found as:

$$\begin{aligned} & D_1 \lambda_i^4 q_i - D_2 \int_0^1 \left[\sum_{j=1}^{N} q_j \frac{\mathrm{d}^6}{\mathrm{d}X^6} \phi_j \right] \phi_i \mathrm{d}x \\ & - \eta \int_0^1 \left[\left(\int_0^1 \left(\sum_{j=1}^{N} q_j \frac{\mathrm{d}\phi_j}{\mathrm{d}x} \right)^2 \mathrm{d}x \right) \sum_{j=1}^{N} q_j \frac{\mathrm{d}^2 \phi_j}{\mathrm{d}x^2} \right] \phi_i \mathrm{d}x \\ & - \int_0^1 \left[\sum_{k=0}^{\infty} A_k \left(\sum_{j=1}^{N} q_j \phi_j \right)^k \right] \phi_i \mathrm{d}x + \mathrm{B.C.} = 0 \qquad i = 1, 2, \ldots, N \end{aligned} \tag{34}$$

where N is the number of considered terms of Rayleigh–Ritz. In above relation, A_k and B.C. are the Taylor expansion coefficient of the external force term and the boundary condition terms, respectively, which are defined as:

$$A_k = \frac{\mathrm{d}^k}{k! \mathrm{d}w^k} \left[\frac{\alpha_m}{(1-w)^m} - \frac{\beta^2 \{2\lambda \cosh(\xi_0(1-w)) - (1+\lambda^2)\}}{2 \sinh^2(\xi_0(1-w))} \right] \Bigg|_{w=0} \tag{35}$$

$$\mathrm{B.C.} = D_2 \frac{\mathrm{d}^3}{\mathrm{d}X^3} \left(\sum_{j=1}^{N} q_j \phi_j \right) \frac{\mathrm{d}^2 \phi_i}{\mathrm{d}X^2} \Bigg|_{x=1} - D_2 \frac{\mathrm{d}^3}{\mathrm{d}X^3} \left(\sum_{j=1}^{N} q_j \phi_j \right) \frac{\mathrm{d}^2 \phi_i}{\mathrm{d}X^2} \Bigg|_{x=0} \tag{36}$$

The obtained system of algebraic equations is solved to obtain q_i value and consequently $w(x)$. The instability occurs when $\mathrm{d}w(x = 0.5)/\mathrm{d}\beta^2 \to 0$. The instability parameters of the system can be determined via the slope of the $w - \beta$ graphs by plotting w versus β.

3.2. Lumped parameter model (LPM)

Lumped parameter models are very beneficial for explaining the physical behavior of systems without mathematical complexity. To obtain a simple model for simulation of the electromechanical behavior of the nanobridge, a lumped parameter model is developed in this subsection. For this purpose, the nanobridge shown in Fig. 1 is replaced by a one-dimensional simple structure which undergoes uniformly distributed loading (Fig. 2). The structure is constructed from a linear spring with stiffness of K. LPM can be developed by minimizing the total energy of the system. The detail of the method is found in "Appendix". Based on LPM, the relation between applied voltage and the maximum deflection of the nanobridge, $w_{\max}$, can be obtained as:

$$\beta^2 = \frac{2 \sinh^2(\xi_0(1-w_{\max})) \left[-\pi^4 w_{\max} \left(4D_1 + 16\pi^2 D_2 + \frac{1}{2} w_{\max}^2 \eta \right) + \alpha_m (1-w_{\max})^{-m} \right]}{2\lambda \cosh(\xi_0(1-w_{\max})) - 1 - \lambda^2} \tag{37}$$

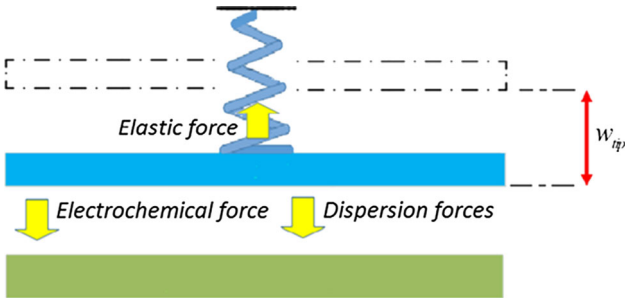

Fig. 2 Lumped parameter model

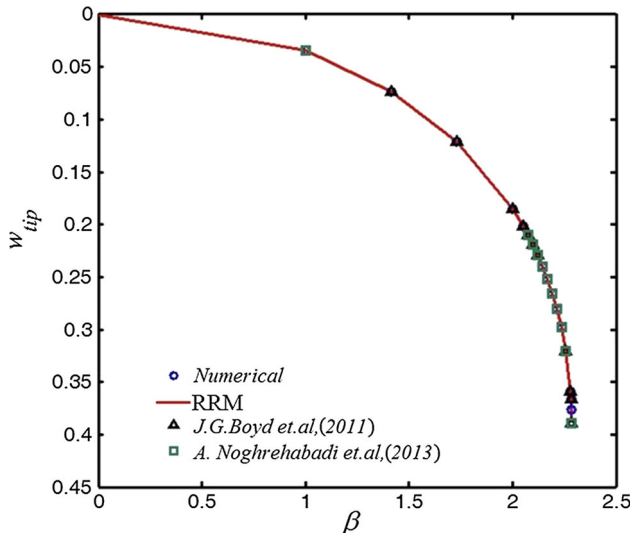

Fig. 3 Variation of the normalized tip deflection as a function of normalized applied voltage

In the case of LPM, the pull-in parameters can be obtained from Eq. (40) by setting $\mathrm{d}\beta^2/\mathrm{d}w_{\max} = 0$.

3.3. Numerical solution method

In addition with the RRM and LPM, the deflection of the nanobridge is numerically simulated using MAPLE software. Utilizing Hamilton principle, i.e., $\delta(\ ) = 0$, in which δ indicates variations symbol, the governing equation of lateral deflection of the system can be derived as the following

$$D_1\frac{\mathrm{d}^4w}{\mathrm{d}x^4} - D_2\frac{\mathrm{d}^6w}{\mathrm{d}x^6} - \eta\left[\int_0^1\left(\frac{\mathrm{d}w}{\mathrm{d}x}\right)^2\mathrm{d}x\right]\frac{\mathrm{d}^2w}{\mathrm{d}x^2} = \frac{\alpha_m}{(1-w)^m} - \frac{\beta^2\left[\lambda\cosh(\xi_0(1-w)) - \frac{1}{2}(\lambda^2+1)\right]}{\sinh^2(\xi_0(1-w))} \tag{38}$$

And the following boundary conditions

$$w(0) = \frac{\mathrm{d}w}{\mathrm{d}X}(0) = \frac{\mathrm{d}^3w}{\mathrm{d}X^3}(0) = w(1) = \frac{\mathrm{d}w}{\mathrm{d}X}(1) = \frac{\mathrm{d}^3w}{\mathrm{d}X^3}(1) = 0 \tag{39}$$

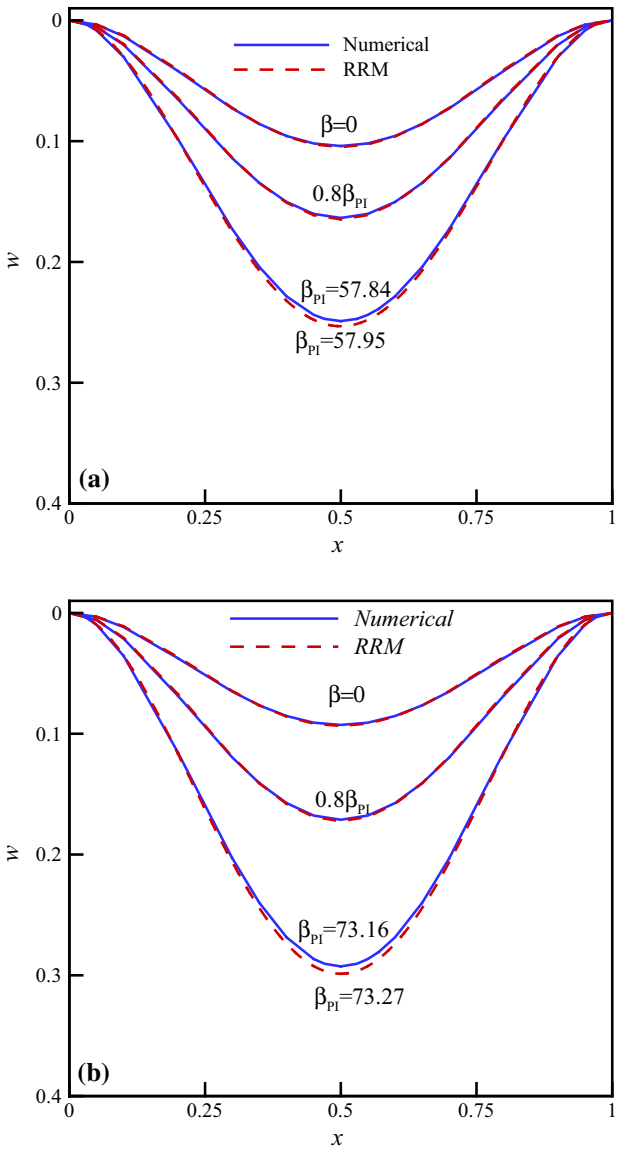

Fig. 4 Deflection of the nanobridge for different values of applied voltage from zero to pull-in voltage; (**a**) Casimir force (**b**) vdW force ($l_0/l_2 = l_1/l_2 = h/l_2 = 1$, $\alpha_m = 500$, $\xi_0 = 1.5$ and $\lambda = 0.1$)

The highly nonlinear integro-differential equation Eq. (38) cannot be solved analytically. Hence the iterative method is used to solve the equation [58]. The step size of the parameter variation is chosen based on the sensitivity of the parameter to the maximum deflection (mid-length deflection). By numerically solving the differential equations, the deflection of the nanobridge is determined. When the instability occurs, no solution exists and the pull-in parameters of the system can be determined by plotting the mid-deflection versus the applied force.

It should be noted that Eq. (38) turns to that of the classical theory, by setting the l_0, l_1 and l_2 equal to zero. Furthermore, the size-dependent behavior of nanobeam

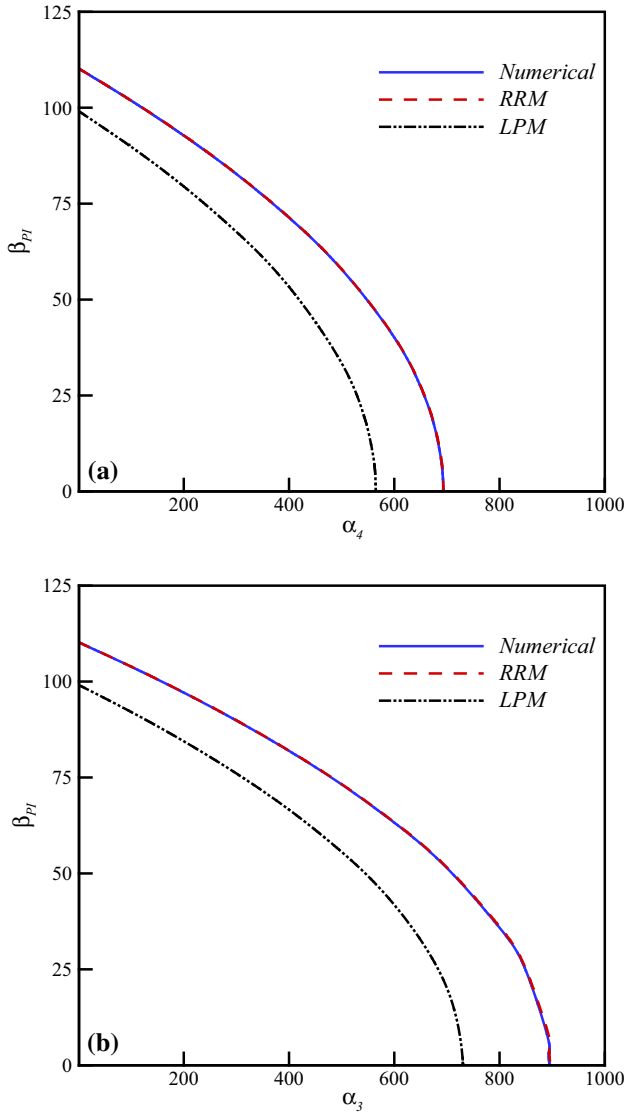

Fig. 5 Effects dispersion force on pull-in voltage deflection (**a**) Casimir and (**b**) vdW for $l_0/l_2 = l_1/l_2 = h/l_2 = 1, \xi_0 = 1.5, \lambda = 0.1$

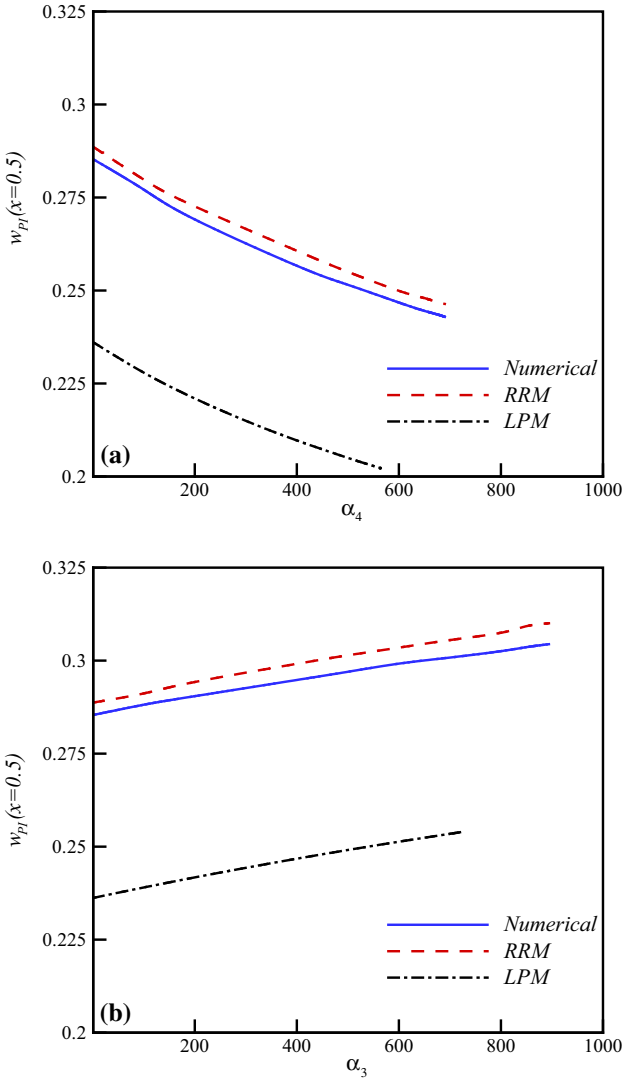

Fig. 6 Effects dispersion forces on pull-in deflection (**a**) Casimir and (**b**) vdW for $l_0/l_2 = l_1/l_2 = h/l_2 = 1$, $\xi_0 = 1.5, \lambda = 0.1$

based on the modified couple stress theory can be obtained by considering $l_0 = l_1 = 0$ and $l_2 = l$.

4. Results and discussion

In the following, typical clamped nanobridge with the geometrical characteristics of $L = 25h$ and $\lambda = 0.1$ are considered. The Young's modulus E, and shear modulus μ are selected as 169 GPa and 65.8 GPa, respectively.

4.1. Comparison with literature

To the best knowledge of the authors, the electromechanical behavior of clamped nanobridge immersed in the ionic liquid electrolyte has not been modeled yet. Indeed, only cantilever configuration is considered by a few researchers [20, 21]. Therefore, in this section a cantilever nanobeam ($\eta = 0$) is simulated using presented model and the obtained results are compared with literature [18, 19]. The governing equation of the cantilever nanobeam was obtained based on classical theory ($l_0 = l_1 = l_2 = 0$) and neglecting dispersion forces. The boundary conditions of

Table 1 Relations for determining the detachment length and minimum gap

Casimir regime	vdW regime
$L_{\max} = \sqrt[4]{\frac{240n\mathrm{EI}g^5\alpha_4^*}{\pi^2 hb}}$	$L_{\max} = \sqrt[4]{\frac{6\pi g^4 \mathrm{EI}\alpha_3^*}{\bar{A}(n)b}}$
$g_{\min} = \sqrt[5]{\frac{\pi^2 hbL^4}{240n\mathrm{EI}\alpha_4^*}}$	$g_{\min} = \sqrt[4]{\frac{\bar{A}(n)bL^4}{6\pi\mathrm{EI}\alpha_3^*}}$

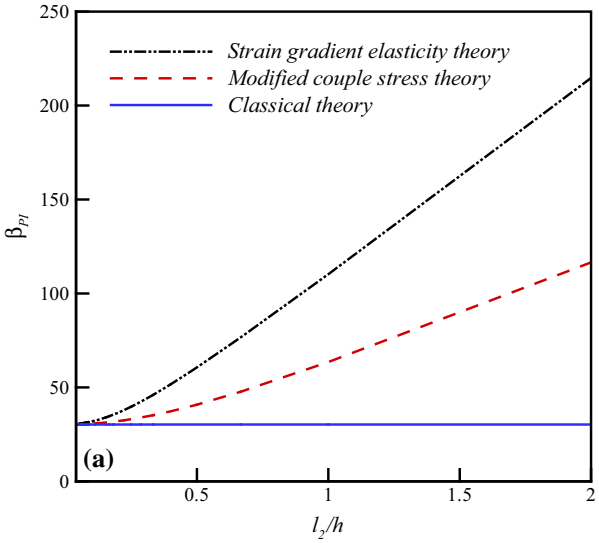

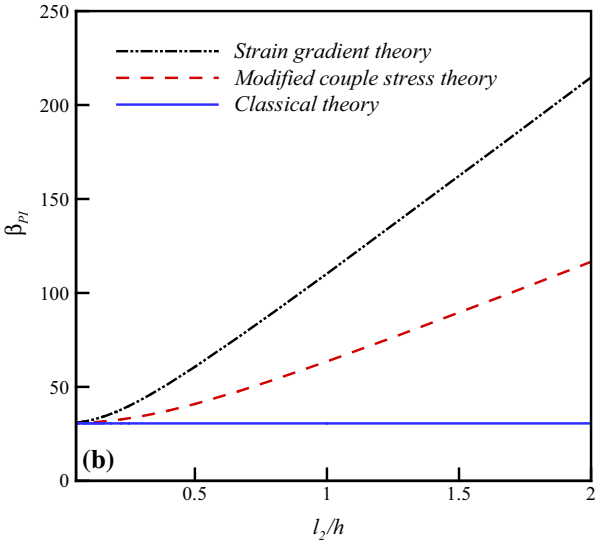

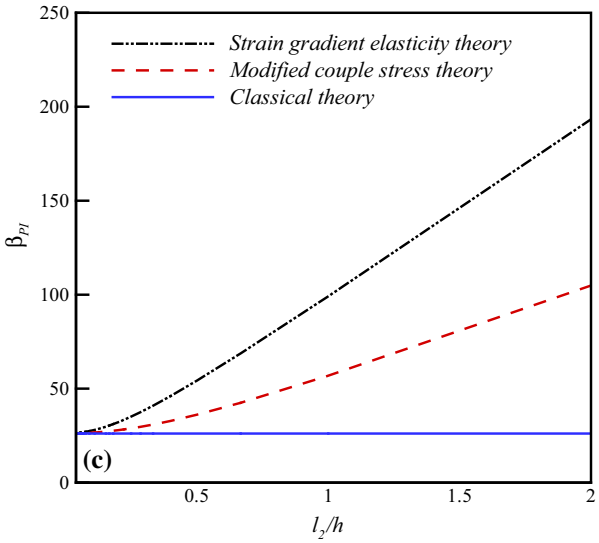

◀**Fig. 7** Pull-in voltage for different models as a function of size effect parameter (l_2/h) and neglecting dispersion forces, (**a**) numerical, (**b**) RRM and (**c**) LPM. $l_0/l_2 = l_1/l_2 = h/l_2 = 1$, $\xi_0 = 1.5$, $\lambda = 0.1$, $\alpha_m = 0$

the cantilever beam is selected the same as Refs. [20, 21]. Figure 3 shows the influences of the normalized applied voltage, β, on the normalized tip deflection, $w(x = 1)$, of the cantilever beam for $\alpha_m = 0, \lambda = 0.1, \xi_0 = 1$. It can be observed that the normalized tip deflection would increase with an increase in the input voltage. This figure reveals that RRM results are in very good agreement with the results of finite element solution [20] and the modified Adomian method [21].

4.2. Deflection and stability

Figure 4 shows the variation of deflection of typical nanobridge when the applied voltage increases from zero to pull-in value. The vertical axis reveals the deflection of the nanobridge, while the horizontal axis reveals the dimensionless length of the beam. As seen, increasing the applied voltage increases the deflection of the nanobridge. When the applied voltage exceeds its critical value, β_{PI}, then no solution exists and the pull-in instability occurs. Note that the operation distance of the system is limited by this instability. This figure shows that the nanobridge has an initial deflection even when no voltage applied which is due to the presence of dispersion forces. It is observed that the results of RRM are in good agreement with those of numerical method. The relative error of presented methods with respect to the numerical solution is <1 %.

4.3. Influence of dispersion forces

If the gap between the beam and the ground is of the order of several nanometers, the effect of dispersion forces must be taken into account. The effect of dispersion forces on the pull-in voltage of the nanobridge—is presented in Fig. 5a, b. As seen, increasing the dispersion forces leads to a decrease in the pull-in voltage of the system. Interestingly, the intersection point of the curves and the horizontal axis corresponds to the critical value of dispersion forces in liquid media; if the nanobeam is close enough to the ground, dispersion forces can induce stiction even without any electrostatic force.

Influence of dispersion on the pull-in deflection (midpoint deflection at pull-in) of the system is presented in Fig. 6a, b. This figure shows that while increase in the Casimir force slightly reduces the pull-in deflection of the nanobridge, increasing the vdW attraction increases the pull-in deflection of the system.

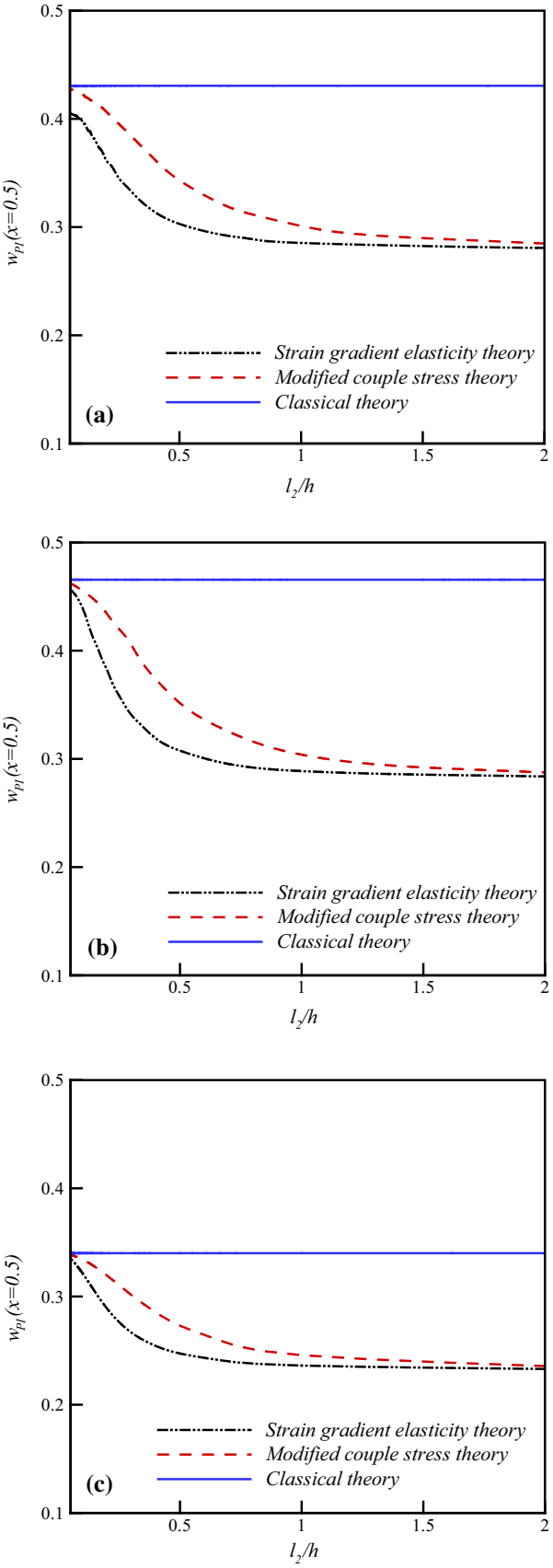

◀**Fig. 8** Pull-in deflection for different models as a function of size effect parameter (l_2/h) and neglecting dispersion forces (**a**) numerical, (**b**) RRM and (**c**) LPM. $l_0/l_2 = l_1/l_2 = 1$, $\xi_0 = 1.5$, $\lambda = 0.1$, $\alpha_m = 0$

As seen in Figs. 5 and 6, the lumped parameter model (LPM) exhibits the same physical trend in comparison with those of numerical solution and RRM. However, some deviations from the numerical and RRM values (error) are observed. Note that the LPM can be considered as a simple technique for rapidly evaluating the qualitative impact of a design parameter on the bridge stability. However, it may not be appropriate for precisely determining the pull-in values.

4.3.1. Detachment length and minimum gap

When the gap between the moveable electrode and the ground is sufficiently small, then even without an applied voltage ($\psi_1 = \psi_2 = 0$), the nanoactuators can adhere to the ground due to the nanoscale attractions. The maximum length of the nanobeam, $L_{\max}$, at which the nanoactuators does not stick to the substrate without the application of a voltage difference is called the detachment length [59, 60]. The detachment length is the maximum permissible length of the freestanding nanobeam. On the other hand, if the length of nanobridge is known, there is a minimum gap, $g_{\min}$, which prevents stiction due to the dispersion forces. The $L_{\max}$ and $g_{\min}$ are very important for reliable operation of nanodevices and can be determined from the critical value of dispersion forces. The critical values of Casimir of vdW force, α_m^*, and the corresponding critical tip deflection, $w_{\text{tip}}^{\text{PI}}$, can be acquired by setting $\beta = 0$ and then plotting $w(x = 1)$ versus α_m. Substituting α_m^* into definition of α_m, one can calculate the values of $L_{\max}$ and $g_{\min}$. Table 1 shows the relations for determining the $L_{\max}$ and $g_{\min}$ values for liquid-immersed nanobridge.

4.4. Influence of size effect

Variation of the pull-in voltage (β_{PI}) of the nanobridge is demonstrated in Fig. 7a–c as a function of size effect parameter, l_2/h for different theories. These figures show that increasing l_2/h results in enhancing the instability voltage of the system. This means size effect provides a hardening behavior that enhances the elastic resistance and consequently pull-in voltage of the nanobridge. On the other hand, with increase in the beam thickness, results of strain gradient theory approaches to those of classic theory (horizontal lines). Figure 8a–c represents the influence of size effect on the instability deflection (w_{PI}) of the nanobridge. As seen, with increasing l_2/h the pull-in deflection of the nanobridge decreases, although in classical theory the pull-in deflection is independent of the size effect.

4.5. Effects of ion concentration

The effect of ion concentration parameter (ξ_0) on the instability behavior of the nanobridge is shown in Fig. 9a, b considering the presence of dispersion forces. This figure reveals that the pull-in voltage enhances by increasing ξ_0. The results of Fig. 9a, b demonstrate that the augmentation of ions in the vicinity of electrodes surface increases the instability voltage. Figure 10a, b shows the effect of ion concentration on the pull-in deflection of the nanobridge. As seen, increase in ion concentration can decrease the pull-in deflection. Indeed, Figs. 9 and 10 reveal that increase in the Debye length of the electrolyte enhances the instability voltage while reduces the maximum stable deflection of the system.

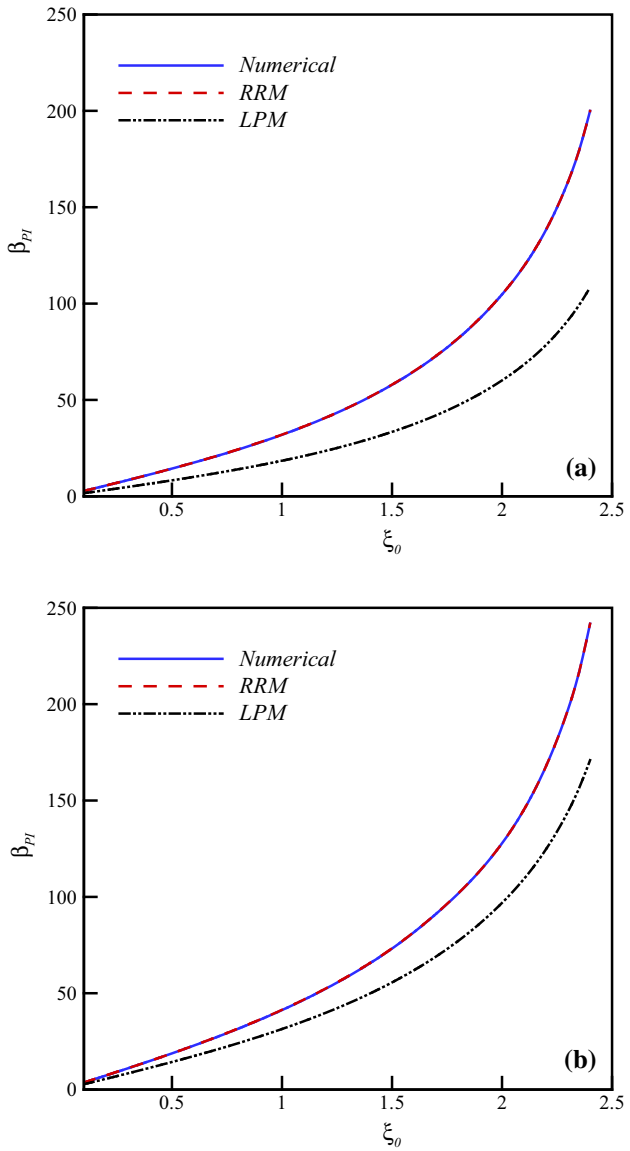

Fig. 9 Effects of ion concentration on the pull-in voltage for $l_0/l_2 = l_1/l_2 = h/l_2 = 1$, $\alpha_m = 500$, $\lambda = 0.1$ (**a**) Casimir and (**b**) vdW

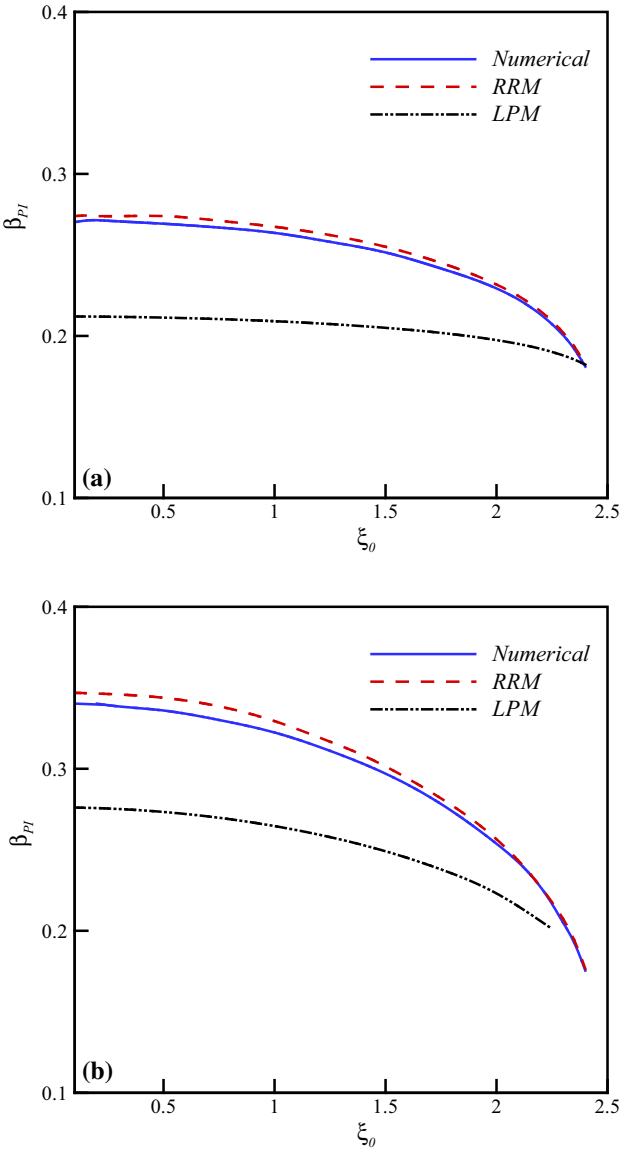

Fig. 10 Effects of ion concentration on the pull-in deflection for $l_0/l_2 = l_1/l_2 = h/l_2 = 1$, $\alpha_m = 500$, $\lambda = 0.1$ (**a**) Casimir and (**b**) vdW

4.6. Effect of potential ratio

Figure 11a, b shows the influence of the potential ratio (λ) on mid-point deflection of the nanobridge for different size parameter values. As seen, mid-point deflection of the double-clamped nanobridge is always positive for any amount of λ value. Note that this trend is different from what observed in cantilever nanobeam where its free-end deflection can be positive or negative depending on λ value [19]. This figure implies that for both repulsive and attractive electrochemical forces, the double-clamped beam deflects downward. This difference is the result of nonlinear stretching term that induces stiffening effect in the nanobridge.

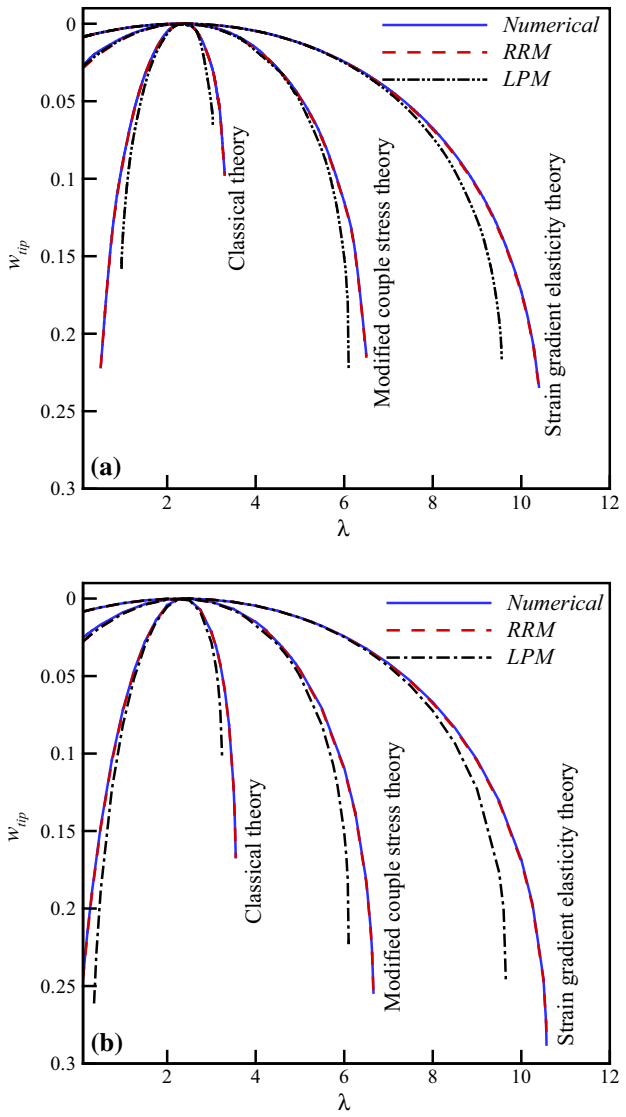

Fig. 11 Influence potential ratio and size effect on normalized mid-deflection (**a**) Casimir (**b**) vdW for $l_0/l_2 = l_1/l_2 = h/l_2 = 1, \xi_0 = 1.5$, $\alpha_m = 50$, $\beta = 10$

5. Conclusions

The strain gradient theory has been employed to investigate the size-dependent pull-in instability of electromechanical nanobridge immersed in liquid electrolyte, considering the effect of electrical double layer and dispersion forces. The nonlinear governing equation has been solved using three different approaches. The obtained results show that the dispersion forces reduce the pull-in voltage of the nanobridge. While Casimir force reduces the pull-in deflection of the nanobridge, vdW attraction increases the instability deflection of the system. For ultra-thin nanobridge that the thickness is comparable with the material length scale parameters, size effect increases the pull-in voltage due to the stiffening effect. It is found that augmentation of bulk ion concentration increases the pull-in voltage of the nanobridge while decreases the pull-in deflection of the system. Nanobridge can only bend down for any potential ratio value. This trend is different from that reported for nanocantilevers. The results obtained using Rayleigh–Ritz method is in good agreement with those of numerical method. The LPM has the advantage of providing simple closed-form approximation for engineers and designers.

Appendix: Lumped parameter model

In order to develop a lumped parameter model, a trial solution for deflection of the nanobridge is selected as the following:

$$W(X) = \frac{W_{\max}}{2}\left(1 - \cos\left(\frac{2\pi X}{L}\right)\right) \tag{40}$$

Taking the derivative from total energy of the system [Eq. (22)] with respect to $W_{\max}$ and setting the result to zero (e.g., $\frac{d\Pi}{dW_{\max}} = 0$), yields the load–deflection characteristic equation:

$$\frac{\pi^4 W_{\max} E}{4L^4}\left(16ID_1 + 64I\pi^2 D_2 + AW_{\max}^2\right) - f_{\text{ext}} = 0 \tag{41}$$

Substituting f_{ext} at $W = W_{\max}$ in the above relation one can obtain:

$$\frac{\pi^4 W_{\max} E(16ID_1 + 64I\pi^2 D_2 + AW_{\max}^2)}{4L^4} + \frac{b\varepsilon\varepsilon_0\kappa^2\psi_1^2\left[2\frac{\psi_2}{\psi_1}\cosh(\kappa(g - W_{\max})) - 1 - \left(\frac{\psi_2}{\psi_1}\right)^2\right]}{2\sinh^2(\kappa(g - W_{\max}))} - \begin{cases} \frac{\bar{A}b}{6\pi(g - W_{\max})^3} \\ \frac{\pi^2\hbar b}{240\sqrt{\tau v}(g - W_{\max})^4} \end{cases} = 0 \tag{42}$$

Using the definition of $w_{\max} = W_{\max}/g$ the dimensionless relation can be written as:

$$\pi^4 w_{\max}\left(4D_1 + 16\pi^2 D_2 + \frac{1}{2}w_{\max}^2\eta\right) + \frac{\beta^2[2\lambda\cosh(\xi_0(1 - w_{\max})) - 1 - \lambda^2]}{2\sinh^2(\xi_0(1 - w_{\max}))} - \frac{\alpha_m}{(1 - w_{\max})^m} = 0 \tag{43}$$

By rearranging Eq. (43), the relation between applied voltage and the maximum deflection can be obtained in the form of Eq. (37).

References

[1] C Ke and H D Espinosa Nanoelectromechanical systems (NEMS) and modeling, in *Handbook of Theoretical and Computational Nanotechnology* (eds.) M Rieth, W Schommers and P D Gennes (Illinois: American Scientific Publishers) Ch 121, p 1 (2006)

[2] J L Muñoz-Gamarra, P Alcaine, E Marigó, J Giner, A Uranga, J Esteve and N. Barniol *Microelectron. Eng*. **110** 246 (2013)

[3] M Dragoman, D Dragoman, F Coccetti, R Plana and A A Muller *J. Appl. Phys*. **105** 054309 (2009)

[4] A Uranga, J Verd, E Marigó, J Giner, J L Muñóz-Gamarra and N Barniol *Sens. Actuators A: Phys*. **197** 88 (2013)

[5] C Hierold, A Jungen, C Stampfer and T Helbling *Sens. Actuators A*. **136** 51 (2007)

[6] H M Sedighi, Changizian M and A Noghrehabadi *Lat. Am. J. Solids Struct*. **11** 810 (2014)

[7] H Sadeghian and G Rezazadeh *Commun. Nonlinear Sci. Numer. Simul*. **14** 2807 (2009)

[8] H M Sedighi, F Daneshmand and M Abadyan *Compos. Struct.* **124** 55 (2015)

[9] H M Sedighi *Int. J. Appl. Mech.* **6**(3) 1450030 (2014)

[10] S Rollier, B Legrand, D Collard and L Buchaillot *J. Micromech. Microeng*. **16** 794 (2006)

[11] O Loh, A Vaziri and H D Espinosa *Exp. Mech*. **49** 105 (2009)

[12] K Oh, J H Chung, S Devasia and J J Riley *Lab Chip* **9** 1561 (2009)

[13] N C Tsai and C Y Sue *Sens. Actuators A* **134** 555 (2007)

[14] J G Boyd and D Kim *J. Colloid Interface Sci*. **301** 542 (2006)

[15] G Gramse, M A Edwards, L Fumagalli and G Gomila *Appl. Phys. Lett.* **101** 213108 (2012)

[16] G Rezazadeh, M Fathalilou, R Shabani, S Tarverdilou and S Talebian *Microsyst. Technol.* **15** 1355 (2009)

[17] T L Sounart, T A Michalske and K R Zavadil *J. Microelectromech. Syst.* **14** 125 (2005)

[18] A Maali, C Hurth, R Boisgard, C Jai, T Cohen-Bouhacina and J P Aimé *J. Appl. Phys.* **97** 074907 (2005)

[19] C Y Yang and Y-P Zhao *J. Chem. Phys.* **120** 5366 (2004)

[20] J G Boyd and J Lee *J. Colloid Interface Sci*. **356** 387 (2011)

[21] A Noghrehabadi, M Eslami and M Ghalambaz *Int. J. Non Linear Mech*. **52** 73 (2013)

[22] E Buks and M L Roukes *Phys. Rev. B* **63** 033402 (2001)

[23] E Buks and M L Roukes *Europhys. Lett*. **54** 220 (2011)

[24] A Farrokhabadi, A Koochi and M Abadyan *Microsyst. Technol.* **20** 291 (2013)

[25] A Noghrehabadi, Y Tadi Beni, A Koochi, A S Kazemi, A Yekrangi, M Abadyan and M Noghrehabadi *Procedia Eng.* **10** 3758 (2011)

[26] A Koochi and M Abadyan *J. Appl. Sci*. **11** 3421 (2011)

[27] J S Duan, R Rach and A M Wazwaz *Int. J. Non-Linear Mech*. **49** 159 (2013)

[28] W H Lin and Y P Zhao *Chin. Phys. Lett*. **20** 2070 (2003)

[29] M Dequesnes, S V Rotkin and N R Aluru *Nanotechnology* **13** 120 (2002)

[30] H M Sedighi H M, F Daneshmand and J Zare *Arch. Civ. Mech. Eng.* **14**(4) 766 (2014)

[31] N A Fleck, G M Muller, M F Ashby and J W Hutchinson *Acta Metall. Mater*. **42** 475 (1994)

[32] J S Stolken and A G Evans *Acta Mater*. **46** 5109 (1998)

[33] D C C Lam, F Yang, A C M Chong, J Wang and P Tong *J. Mech. Phys. Solids.* **51** 1477 (2003)

[34] B Wang, S Zhou, J Zhao and X Chen *J. Micromech. Microeng*. **21** 027001 (2011)

[35] B Wang, S Zhou, J Zhao and X Chen *Int. J. Precis. Eng. Manuf*. **12** 1085 (2011)

[36] B Wang, S Zhou, J Zhao and X Chen *Int. J. Appl. Math*. **4** 1250003 (2012)

[37] R Ansari, R Gholami, V Mohammadi and M Faghih Shojaei *Compos. Struct*. **95** 430 (2013)

[38] V Mohammadi, R Ansari, M Faghih Shojaei, R Gholami and S Sahmani *Nonlinear Dyn*. **73** 1515 (2013)

[39] M Fathalilou, M Sadeghi and G Rezazadeh *J. Mech. Sci. Technol*. **28** 1141 (2014)

[40] A Koochi, H M Sedighi and M Abadyan *Lat. Am. J. Solids Struct*. **11** 1806 (2014)

[41] H M Sedighi, A Koochi and M Abadyan *Int. J. Appl. Mech*. **6** 1450055 (2014)

[42] H M Sedighi *Acta Astronaut.* **95** 111 (2014)

[43] K W McElhaney, J J Valssak, W D Nix *J. Mater. Res.* **13** 1300 (1998)

[44] W D Nix and H Gao *J. Mech. Phys. Solids* **46** 411 (1998)

[45] A C M Chong and D C C Lam *J. Mater. Res.* **14** 4103 (1999)

[46] Y Cao, D D Nankivil, S Allameh, W O Soboyejo *Mater. Manuf. Process.* **22** 187 (2007)

[47] R K A Al-Rub and G Z Voyiadjis *Int. J. Multiscale Comput. Eng.* **2** 377 (2004)

[48] W Wang, Y Huang, K J Hsia, K X Hu, A Chandra *Int. J. Plast.* **19** 365 (2003)

[49] R Maranganti and P Sharma *J. Mech. Phys. Solids* **55** 1823 (2007)

[50] K T Chan and Y P Zhao *Sci. Chin. Phys. Mech. Astron.* **54** 1854 (2011)

[51] M R Ghazavi, G Rezazadeh, S Azizi *Sens. Transducers J*. **103** 132 (2009)

[52] L P Teo *Phys. Rev. A* **81** 032502 (2010)

[53] J N Israelachvili *Intermolecular and Surface Forces* (USA: Academic Press) Ch 13 p 253 (2011)

[54] G L Klimchitskaya, U Mohideen and V M Mostepanenko *Phys. Rev. A*. **61** 062107 (2000)

[55] M Bostrom and B E Sernelius *Phys. Rev. B* **61** 2204 (2000)

[56] J N Israelachvili and D Tabor *Proc R. Soc. A*. **331** 19 (1972)

[57] H M Sedighi and K H Shirazi *Acta Astronaut.* **85** 19 (2013)

[58] R Dargazany, K Hörnes and M Itskov *Appl. Math. Comput.* **221** 833 (2013)

[59] W H Lin and Y P Zhao *Chaos Solitons Fract.* **23** 1777 (2003)

[60] W H Lin and Y P Zhao *Microsyst. Technol.* **11** 80 (2005)